

unpolluted. Like the  $O_3$  measurements shown in Fig. 3, the  $NO_2$  measurements also reveal a decrease near day 40 to 42 when the center of the geopotential low was nearest to Thule, as indicated in Fig. 3, suggesting that the  $NO_2$  abundances near the center of Arctic vortex are less than those outside. This result supports the assertion that these data are dominated by stratospheric  $NO_2$  rather than tropospheric pollution.

The observed values and upper limits for  $NO_2$  shown in Figs. 4 and 5 are extremely low. They are as low and lower than the Antarctic measurements during August at McMurdo Station (3, 4, 9). For comparison, two-dimensional model calculations (11) predict a total  $NO_2$  column of  $1.5 \times 10^{15} \text{ cm}^{-2}$  at the end of January and  $2.0 \times 10^{15} \text{ cm}^{-2}$  at the end of February for  $75^\circ\text{N}$ . Thus these observations suggest that a significant depletion of stratospheric  $NO_2$  had occurred at Thule during the winter of 1988. This result is not particularly surprising in view of the extreme low temperatures over Thule during this period and in view of theoretical and observational studies of  $HNO_3$  suggesting that nitrogen radical species are converted to  $HNO_3$  during the polar winter (12), probably through heterogeneous chemistry. Further interpretation of such observations requires detailed consideration of the past history of the air parcels over Thule so that the formation and destruction of  $N_2O_5$  can be evaluated, as well as the frequency and chemistry of PSCs.

Few in situ measurements of nitrogen radical species in winter at high latitudes are available. Balloon-borne measurements reveal  $NO$  and  $NO_2$  mixing ratios of about 60 to 100 parts per trillion by volume (pptv) and 100 to 150 pptv, respectively, from 15 to 22 km (13) in western Canada under relatively warm winter conditions (that is, temperatures of  $-50^\circ$  to  $-60^\circ\text{C}$  from 15 to 30 km). Thus these measurements were conducted under much warmer conditions and much farther from the center of the Arctic vortex than the observations reported here. Simultaneous ground-based measurements of the total  $NO_2$  column during the period of those observations range from about  $0.7 \times 10^{15}$  to  $2.0 \times 10^{15} \text{ cm}^{-2}$  (13). The latter values were typical of afternoon twilights and are significantly greater than the evening twilight values measured here. The low total column  $NO_2$  measurements at Thule thus suggest that the abundances of lower stratospheric  $NO_x$  were likely well below 60 pptv, which is consistent with the assertion that the observation of nighttime OClO abundances of about  $5 \times 10^{13} \text{ cm}^{-2}$  as presented in (2) imply  $NO_2$  mixing ratios of only a few parts per trillion by volume in

the lower stratosphere. These considerations, together with the observation that  $NO_2$  levels over Thule were even lower than our measurements performed at McMurdo Station, Antarctica, suggest that heterogeneous chemistry plays an important role in determining the abundance of nitrogen and chlorine species during cold Arctic winters.

#### REFERENCES AND NOTES

1. J. C. Farman, B. G. Gardiner, J. D. Shanklin, *Nature* **315**, 207 (1985).
2. S. Solomon, G. H. Mount, R. W. Sanders, R. O. Jakoubek, A. L. Schmeltekopf, *Science* **242**, 550 (1988).
3. G. H. Mount, R. W. Sanders, A. L. Schmeltekopf, S. Solomon, *J. Geophys. Res.* **92**, 8320 (1987).
4. R. L. McKenzie and P. V. Johnston, *Geophys. Res. Lett.* **11**, 73 (1984); C. B. Farmer, G. C. Toon, P. W. Shaper, J. F. Blavier, L. L. Lowes, *Nature* **329**, 126 (1987).
5. J. M. Russell *et al.*, *J. Geophys. Res.* **89**, 5099 (1984).
6. W. P. Chu and M. P. McCormick, *ibid.* **91**, 5465 (1986); J. M. Zawodny, *ibid.*, p. 5439.
7. J. F. Noxon, E. C. Whipple, Jr., R. S. Hyde, *ibid.* **84**, 5047 (1979); J. F. Noxon, *ibid.*, p. 5067; J. F. Noxon, E. Marovich, R. B. Norton, *ibid.*, p. 7883 (1979); J. F. Noxon, *ibid.* **85**, 4560 (1980); J. F. Noxon, W. R. Henderson, R. B. Norton, *ibid.* **88**, 5240 (1983).
8. M. T. Coffey, *Geophys. Res. Lett.* **15**, 331 (1988).
9. S. Solomon, A. L. Schmeltekopf, R. W. Sanders, *J. Geophys. Res.* **92**, 8329 (1987); R. W. Sanders, S. Solomon, M. A. Carroll, A. L. Schmeltekopf, *ibid.*, in press.
10. R. R. Dickerson, *J. Geophys. Res.* **90**, 10739 (1985).
11. R. R. Garcia and S. Solomon, *ibid.* **88**, 1379 (1983); S. Solomon, R. R. Garcia, F. Stordal, *ibid.* **90**, 12981 (1985).
12. S. C. Wofsy, *ibid.* **83**, 364 (1978); J. Austin, R. R. Garcia, J. M. Russell, S. Solomon, A. F. Tuck, *ibid.* **91**, 5477 (1986).
13. B. A. Ridley *et al.*, *ibid.* **92**, 11919 (1987).
14. This research would not have been possible without close collaboration with J. Meriwether and the University of Michigan, Ann Arbor. We also appreciate the kind permission of the Danish government. Critical support by T. Coonrod and other IIT personnel, along with N. Watson and other USAF personnel and R. Kollyer and K. Walsh, is also gratefully acknowledged.

8 July 1988; accepted 15 August 1988

## In Situ Northern Mid-Latitude Observations of ClO, $O_3$ , and BrO in the Wintertime Lower Stratosphere

W. H. BRUNE,\* D. W. TOOHEY, J. G. ANDERSON, W. L. STARR, J. F. VEDDER, E. F. DANIELSEN

In order to test photochemical theories linking chlorofluorocarbon derivatives to ozone ( $O_3$ ) depletion at high latitudes in the springtime, several related atmospheric species, including  $O_3$ , chlorine monoxide (ClO), and bromine monoxide (BrO) were measured in the lower stratosphere with instruments mounted on the NASA ER-2 aircraft on 13 February 1988. The flight path from Moffett Field, California ( $37^\circ\text{N}$ ,  $121^\circ\text{W}$ ), to Great Slave Lake, Canada ( $61^\circ\text{N}$ ,  $115^\circ\text{W}$ ), extended to the center of the polar jet associated with but outside of the Arctic vortex, in which the abundance of  $O_3$  was twice its mid-latitude value, whereas BrO levels were 5 parts per trillion by volume (pptv) between 18 and 21 kilometers, and 2.4 pptv below that altitude. The ClO mixing ratio was as much as 65 pptv at  $60^\circ\text{N}$  latitude at an altitude of 20 kilometers, and was enhanced over mid-latitude values by a factor of 3 to 5 at altitudes above 18 kilometers and by as much as a factor of 40 at altitudes below 17 kilometers. Levels of ClO and  $O_3$  were highly correlated on all measured distance scales, and both showed an abrupt change in character at  $54^\circ\text{N}$  latitude. The enhancement of ClO abundance north of  $54^\circ\text{N}$  was most likely caused by low nitrogen dioxide levels in the flight path.

**T**RACE CONSTITUENTS IN THE POLAR regions of the stratosphere have until recently received little attention, partly because the photochemical processes there were thought to be negligible compared with the better illuminated mid-lati-

tudes, and partly because observing platforms for trace species have only rarely sampled there. The discovery of the rapid  $O_3$  depletion over Antarctica in the austral spring (1) has focused attention on the interaction between photochemistry and transport of trace species at high southern latitudes. Initially the discussion about the mechanism for  $O_3$  depletion centered on either a chemical (actual  $O_3$  loss) or dynamical ( $O_3$  redistribution) cause (2). However, results from ground-based observing missions to Antarctica, NOZE I (3) in 1986 and NOZE II (4) in 1987, and from the Airborne Antarctic Ozone Experiment

W. H. Brune, D. W. Toohey, J. G. Anderson, Department of Chemistry and Department of Earth and Planetary Sciences, Harvard University, Cambridge, MA 02138.

W. L. Starr, J. F. Vedder, E. F. Danielsen, NASA Ames Research Center, Moffett Field, CA 94035.

\*Present address: Department of Meteorology, Pennsylvania State University, University Park, PA 16802.

(AAOE) mission (5) in 1987, clearly demonstrated that gas-phase catalytic processes involving chlorine are responsible for most of the O<sub>3</sub> loss, but that atmospheric dynamics create the environment necessary for O<sub>3</sub> destruction. The discussion now centers on how the interplay between photochemistry and dynamics works, what the exact photochemical mechanisms are, and how O<sub>3</sub> depletion fits into the global picture.

The basic scenario for O<sub>3</sub> depletion in the Antarctic ozone hole is now known, although many issues remain unresolved. During the winter, air descends into the polar region and temperatures inside the wintertime polar vortex fall below -80°C. Polar stratospheric clouds (PSCs), which are continually being formed at these temperatures during the winter and early spring, play a critical role in the conditioning of the trace gas constituents (6). First, odd-nitrogen compounds, which normally moderate halogen and odd-hydrogen chemistry, are removed from the gas phase and bound up mainly as HONO<sub>2</sub> · 3H<sub>2</sub>O in the PSC aerosol. Odd nitrogen and water vapor then are presumably removed from the lower stratosphere between ~14- and ~22-km altitude when the aerosol particles grow large enough to settle out. Second, chlorine that is normally in the form of HCl and ClONO<sub>2</sub> is converted by heterogeneous reactions on the PSCs to photolytically labile chlorine compounds, such as Cl<sub>2</sub> and HOCl. In the spring, when the stratosphere is again sunlit, these compounds are converted to atomic chlorine, and ozone-destroying catalysis begins. The primary cycle involves the rapid formation of ClO by the reaction between Cl and O<sub>3</sub>, followed by the formation of ClOOCl, a form of the ClO dimer, and its subsequent photolysis (7). Two other cycles also contribute; one involves the reaction between ClO and BrO to form Br and Cl atoms (8), and the other involves the reaction between ClO and HO<sub>2</sub> to form HOCl that is subsequently photolyzed (9). These cycles run unchecked by odd nitrogen until the breakdown of the vortex and the warming of the stratosphere in the spring. The amount of O<sub>3</sub> lost is very sensitive to the number of sunlit days during which the vortex remains cold and intact.

Do similar conditions exist for the high latitudes in the Northern Hemisphere? Certainly no large loss of O<sub>3</sub> in the early spring has been observed, although a 6% decrease in wintertime O<sub>3</sub> from 1979 to 1987 has been deduced from data collected by the SBUV instrument on the Nimbus-7 satellite (10). Also, a clear difference exists in the atmospheric dynamics near the two poles such that the northern vortex is much less stable, conditions are in general warmer,

and the final breakdown of the vortex occurs much earlier (11). All of these factors act to impede the preconditioning of the atmospheric species and to allow a much shorter time for chlorine catalytic processes to operate unrestricted by an influx of odd-nitrogen-rich air. However, the temperature is often low enough that PSCs form (12). Furthermore, in the early spring for the years 1977 through 1979, Noxon (13) and Ridley *et al.* (14) observed low levels of NO<sub>2</sub> and NO over North America as far south as ~50°N. In another measurement, from Thule, Greenland, in February 1988, Mount *et al.* (15) observed NO<sub>2</sub> column abundances in the Arctic polar vortex that were as low as, or lower than, those seen in the Antarctic polar vortex. More evidence that the heterogeneous removal of odd nitrogen and dramatic enhancement of chlorine over Antarctica also occurs over the Arctic comes from the total absorption column measurements by Solomon *et al.* (16) of OCIO from Thule, Greenland, in 1988. The column OCIO was only 5 times smaller than observed values in Antarctica and 50 times greater than the upper limit placed on the mid-latitude column. All of the evidence indicates that the same photochemical processes occur at both poles. Depletion of O<sub>3</sub> in the north is probably moderated by the patchy distribution of air containing low levels of odd nitrogen and high levels of reactive chlorine and by the short amount of time these air masses remain unmixed with NO<sub>2</sub>-rich air.

We report the in situ measurement of a number of trace gases in the lower stratosphere very near the Arctic polar vortex. Observations made simultaneously by instruments mounted on the NASA ER-2 high-altitude aircraft, which is based at Moffett Field, California, are reported for ClO, O<sub>3</sub>, and BrO. The total instrument complement, a subset of that used for the AAOE mission, included the Ames Research Center O<sub>3</sub> photometer, the NCAR-Ames whole air sampler, the Harvard University ClO-BrO instrument, and the navigational aids that are a normal part of the aircraft operation. Results from the whole air sampler will be presented elsewhere (17). A brief explanation of the O<sub>3</sub> and ClO instruments follows.

The Ames Research Center O<sub>3</sub> photometer (18), mounted in the aircraft fuselage just aft of the cockpit, measured the ultraviolet (UV) absorption by O<sub>3</sub> of a mercury lamp emission line at 253.7 nm. Air was driven by dynamic pressure into the system through an inlet mounted underneath the fuselage, and passed through a 70-cm-long absorption cell before being exhausted. Periodically, the air continuously flowing into the absorption cell was sent through a cata-

lytic converter (manganese dioxide-coated copper screens) to remove all of the O<sub>3</sub> from the air. The O<sub>3</sub> content of the air sample was calculated by Beer's Law using the signals with and without O<sub>3</sub> in the path, the path-length, and the absorption cross section. Pressure and temperature of the air in the cell were measured to determine the O<sub>3</sub> mixing ratio. For this instrument, the accuracy of the measurements, including both systematic and random error, was ±3%, and the minimum detectable mixing ratio was ~25 ppbv at 20 km for a 1-s integration time. The O<sub>3</sub> photometer also measured and recorded at a 0.2-Hz rate the total air temperature, Mach number, and ambient pressure, so that potential temperature and pressure altitude could be determined throughout the flight.

The ClO-BrO instrument (19), mounted in the left wing pod of the aircraft, permitted simultaneous detection of ClO and BrO in a decelerated, laminar airstream. The ClO and BrO levels were measured at two different points along the instrument flow tube when reagent NO, added to the ambient airstream, converted the molecules to their respective atoms. The Cl and Br atoms were then detected by resonance fluorescence, in which UV emissions from low-pressure helium discharges containing a trace of Cl or Br were resonantly scattered by Cl or Br atoms in the airstream. The resonantly scattered emissions were detected by photomultipliers set at right angles to both the light source and the air flow. The difference between the signals when NO was added and when it was not was proportional to the ClO or BrO concentration. For ClO, the accuracy of the laboratory and in-flight calibrations was ±25%, and a ClO mixing ratio of 2.5 pptv could be detected at 20-km altitude with a signal-to-noise ratio of 2 in a 32-s period. For BrO, the accuracy was ±35%, and 2.0 pptv of BrO could be detected at 20 km with a signal-to-noise ratio of 2 in 40 min. The accuracies of the instrument calibrations were obtained by combining estimates of the accuracies of all the parameters that affect the calibrations (19).

As important as the instruments was the ability to determine where and when the Arctic polar vortex would be within aircraft flight range of Moffett Field. This particular flight was one part of a series of four flights designed to study the distribution and photochemistry of reactive halogens in the lower stratosphere. Although the center of the vortex normally resides offset from the pole near 0° longitude because of the stratospheric anticyclone over Alaska, this flight series provided an opportunity to attempt the study of the vortex. Since an untimed flight

into the vortex from Moffett Field has a low probability of success, the forecasting was particularly essential. For prediction, we obtained forecast maps of the geopotential heights at the 50-mbar pressure level for 2, 4, 6, and 8 days in advance of the flight from the European Center for Medium Range Forecasting. These forecasts were checked against National Meteorological Center (NMC) analyses of geopotential heights and temperatures at the 50- and 70-mbar levels and were found to be quite accurate for our purposes.

Based on this information, the ER-2 aircraft was sent from Moffett Field to Great Slave Lake on 13 February 1988. The flight trajectory superimposed on a map of the NMC analysis of winds at the 50-mbar level (Fig. 1) indicates that the aircraft crossed the high-wind region of the vortex to the middle of the polar jet. The ambient temperatures along the flight track were always between  $-60^{\circ}$  and  $-70^{\circ}\text{C}$ . Shown in Fig. 2A is the altitude profile of the aircraft, in which the time of flight is given at the bottom of the figure and the latitude at the top. The profile consists of a rapid ascent following take-off to  $\sim 20$  km, a slight increase in altitude until the ER-2 was at  $54^{\circ}\text{N}$  latitude, descent to level flight at 18.3 km for 25 min, followed by descent to 15.3 km, level flight for 5 min, and rapid ascent to maximum altitude. The aircraft was turned southward at a latitude of  $61^{\circ}\text{N}$  and an altitude of 20.0 km and flown to  $38^{\circ}\text{N}$  latitude with an increase to 21.3-km altitude. The solar zenith angle along the flight track varied from  $59^{\circ}$  at Moffett Field to  $79^{\circ}$  at the northernmost point. On the southward leg, the solar zenith angle remained at  $\sim 79^{\circ}$  to  $45^{\circ}\text{N}$  latitude and increased to  $87^{\circ}$  at  $38^{\circ}\text{N}$  latitude just prior to descent at Moffett Field.

The potential temperature along the flight track is shown in Fig. 2B; the  $\text{O}_3$ , ClO, and BrO mixing ratios are shown in Fig. 2, C, D, and E, respectively. Data for  $\text{O}_3$ , reported once a second, are averaged for 32 s to match the data rate of the ClO instrument, and BrO is averaged for 20 to 80 min.

The mixing ratios of ClO,  $\text{O}_3$ , and BrO all increased with both altitude and latitude along the flight track. The ClO mixing ratio reached a peak value of 65 pptv at 20-km altitude and  $60^{\circ}\text{N}$  latitude and has a broad plateau of 55 pptv that extends from the northernmost point in the flight to  $54.2^{\circ}\text{N}$  latitude. When the aircraft flew at 15-km altitude near  $60^{\circ}\text{N}$ , the ClO mixing ratio fluctuated rapidly between 2 and 12 pptv and had an average value of 7 pptv. The structure of the BrO mixing ratio along the flight track mimicked that of ClO, but the variation of BrO was small—where the air-

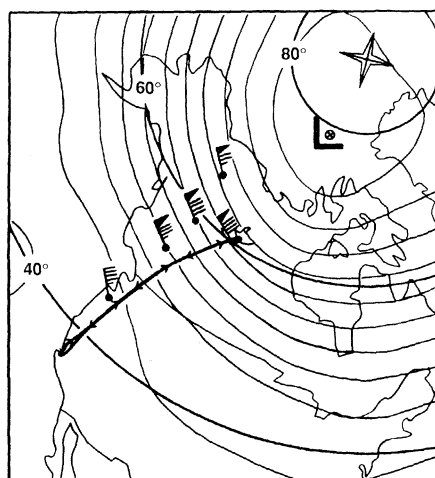


**Fig. 1.** Flight path of the ER-2 aircraft (heavy line with arrowheads) superimposed on a map of the NMC analysis for 13 February 1988 of the wind speeds and geopotential heights on the 50-mbar pressure surface.

craft was above 19-km altitude, the BrO mixing ratio was between 4.0 and 5.2 pptv. During the low-altitude flight near 15-km altitude, the BrO mixing ratio decreased to 2.4 pptv. The  $\text{O}_3$  mixing ratio reached a peak of 4.5 ppmv, and maintained a broad plateau of 4.0 to 4.5 ppmv above 20-km altitude between  $61^{\circ}\text{N}$  and  $54.2^{\circ}\text{N}$  latitudes. The altitude profile of  $\text{O}_3$  taken at  $61^{\circ}\text{N}$  latitude agrees with those measured by Ridley *et al.* (14) for  $54^{\circ}\text{N}$  latitude during February of 1977, 1978, and 1979. For other portions of the flight,  $\text{O}_3$  remained between 1.0 and 4.0 ppmv above 15-km altitude.

A striking feature of these data is the high positive correlation between ClO and  $\text{O}_3$  on all length scales, from 10 to 1000 km. The only deviation from this relation was during the southward leg, most noticeably south of  $55^{\circ}\text{N}$  latitude; ClO was decaying relative to  $\text{O}_3$  because the solar insolation was changing during sunset and ClO was reacting with  $\text{NO}_2$  to form  $\text{ClONO}_2$ , its nighttime reservoir. Both ClO and  $\text{O}_3$  show two steep changes in mixing ratio without a substantial change in aircraft altitude. The first, at 19:55 GMT, resulted from a sudden increase in the potential temperature, indicating the descent of air from higher in the stratosphere to this altitude. The second step occurred at 23:15 GMT, or near  $54.2^{\circ}\text{N}$  latitude, and was not accompanied by a shift in the potential temperature. If we assume that this feature was associated with motion of air around the polar vortex, the northbound leg should show a sudden change at about the same latitude as well. In fact, a steep increase in ClO and  $\text{O}_3$  is evident during the descent of the aircraft to 18 km, at 21:05 GMT. This change in radical mix-

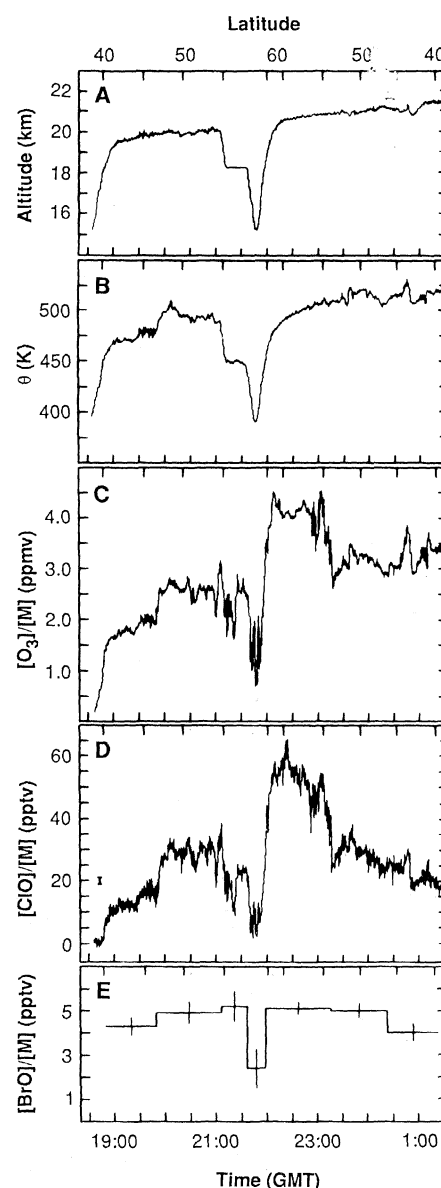


**Fig. 2.** Data obtained during the flight plotted against GMT time and latitude for: (A) aircraft altitude (km); (B) potential temperature (K); (C)  $\text{O}_3$  (ppmv); (D) ClO in pptv; and (E) BrO in pptv. Vertical bars in (D) and (E) represent abundances detectable with a signal-to-noise ratio of 2.

ing ratios corresponds to a sudden increase in potential vorticity (20). Northward of these steep gradients in radical abundances, the mixing ratios of both ClO and  $\text{O}_3$  were larger for a given potential temperature than they were south of the gradients. The air north of  $54.2^{\circ}\text{N}$  latitude was distinctly different from the air south of that latitude.

The purpose of this experiment was to see if the photochemical processes that allow rapid destruction of  $\text{O}_3$  by chlorine catalysis in the Antarctic polar vortex were also occurring in the Arctic polar vortex. The results of this experiment provide no clear answer to that question because the aircraft

**Table 1.** Comparison of altitude profiles for ClO mixing ratio (pptv) at 60°N (February) and 37°N (July).

Latitude	Altitude						
	15	16	17	18	19	20	20.7
60°N	6.9	8.2	9.6	20.3	37.7	52.0	60.0
37°N	<0.2	<0.2	0.5	2.6	5.0	11.0	18.0

did not enter the Arctic polar vortex and only penetrated to the center of the high wind region surrounding the vortex. Nonetheless, the chlorine radical ClO abundance measured at 60°N latitude during this flight was considerably elevated over observed mid-latitude values, as shown in Table 1. The ratio of the ClO abundance at 60°N to that at 40°N was between 3 and 5 at altitudes above 20 km, and increased with decreasing altitude to a value of 40 at altitudes below 17 km. The mid-latitude profile chosen for this comparison was obtained on 30 July 1987 (21), but other profiles during this February series were not, on average, significantly different. If we compare ClO mixing ratios on potential temperature surfaces instead of altitude surfaces, approximately the same enhancement results.

The air mass containing enhanced ClO abundances north of 54°N latitude had descended from higher in the stratosphere. The abundance of O<sub>3</sub> at these latitudes and altitudes serves as an indicator of air motion. The mixing ratio of O<sub>3</sub>, which has its origins in the stratosphere, was approximately a factor of 2 greater than its typical mid-latitude value when compared on either altitude or potential temperature surfaces for the entire altitude interval sampled—15 to 21 km. This increase in O<sub>3</sub> levels indicates that the air mass north of 54°N latitude had descended from at least a few kilometers higher in the stratosphere, in agreement with the measurements of stable gases such as N<sub>2</sub>O, CFC-11, and CFC-12 taken on this same flight (17). Descent of air into the Arctic polar region has also been noted by Ridley *et al.* (14) for February for the years 1977 to 1979 at 54°N, and by Schmidt *et al.* (22) for February 1988 at 68°N.

The descent of air from higher in the stratosphere was, however, not sufficient to cause the observed ClO abundances of 60 pptv. Such air contains more inorganic chlorine, less methane, and more O<sub>3</sub>—all of which favor a larger ClO abundance—but it also contains more reactive nitrogen as NO and NO<sub>2</sub>. This increased reactive nitrogen, when exposed to the faster termolecular reaction rates at the lower altitudes, acts to divert chlorine from ClO to HCl and ClONO<sub>2</sub>. The net result is that the ClO abundance may increase only slightly, or

actually decrease, as the air mass descends. In agreement with this qualitative picture, a two-dimensional model simulation that contained standard photochemistry and dynamics produced ClO abundances at 60°N that were only one-third of the observed values (23). This same simulation, however, was able to reproduce the observed ClO abundances at 37°N latitude. Although this absolute difference at 60°N should be interpreted with some caution, since two-dimensional models produce less downward motion into polar vortices than is observed, the downwelling of air from even higher altitudes cannot by itself explain the large ClO mixing ratios observed.

We are drawn to the conclusion that ClO was observed with a mixing ratio of 50 to 60 pptv because the NO<sub>2</sub> abundance was low over the flight path north of 54°N latitude. The maximum amount of NO<sub>2</sub> consistent with a ClO mixing ratio of 60 pptv is ~60 pptv, as estimated from the results of a zero-dimensional model. This NO<sub>2</sub> abundance is less than the estimates by Ridley *et al.* (14) of more than 100 pptv for their flights at 54°N under similar atmospheric conditions.

Two possibilities are most likely for the low NO<sub>2</sub> abundances in the sampled air mass. First, the air mass may have been advected from a region where PSCs at cold temperatures could have at least partially removed odd-nitrogen compounds. Inside the vortex at Thule, Greenland, in early February 1988, lower stratospheric temperatures were certainly less than -80°C, the NO<sub>2</sub> column abundance was as low as it had ever been observed (15), and the elevated OCIO column abundance and diurnal behavior implied NO<sub>2</sub> mixing ratios in the lower stratosphere of no more than a few parts per trillion by volume (16). Such low levels of NO<sub>2</sub> are a sufficient condition to produce the observed ClO abundances without any conversion of HCl or ClONO<sub>2</sub> on PSCs to chemical precursors of ClO, although the heterogeneous conversion of chlorine species may well occur. A second possibility is that the observed air mass never experienced the extremely low temperatures necessary for heterogeneous removal of the odd-nitrogen compounds. Instead, the low NO<sub>2</sub> could result from a mechanism similar to that suggested for the

Noxon cliff phenomenon (14), in which the NO<sub>2</sub> is sequestered, possibly into N<sub>2</sub>O<sub>5</sub>, in the polar night and then advected to the lower latitudes before N<sub>2</sub>O<sub>5</sub> undergoes significant photolysis. Results from a zero-dimensional photochemical model indicate that enhanced ClO is possible for the scenario with all of the NO<sub>2</sub> initially bound into N<sub>2</sub>O<sub>5</sub> and all of the ClO into ClONO<sub>2</sub> if the air could be advected from the darker, colder region in about a day. If the NO<sub>2</sub> was bound into HNO<sub>3</sub> instead of N<sub>2</sub>O<sub>5</sub>, then NO<sub>2</sub> would remain sufficiently low for air that had been advected from the darker, colder region in about 3 days. Based on our data alone, we cannot determine which of these possible methods of NO<sub>2</sub> reduction is correct.

The lower stratospheric air mass sampled during this experiment north of 54°N latitude was probably depleted in NO<sub>2</sub> and certainly enriched in ClO when compared with air masses at mid-latitudes, just as was the air inside the Arctic polar vortex (15, 16). Under these circumstances, two halogen catalytic cycles, one involving the reaction between ClO and O atoms and the other involving the reaction between ClO and BrO, were major loss mechanisms for O<sub>3</sub>. Which one was larger depended on the time of year and the latitude, since the production of oxygen atoms is a sensitive function of the solar zenith angle and would be greater at lower latitudes. The ClO dimer mechanism, which is mainly responsible for the rapid loss of O<sub>3</sub> in the springtime Antarctic polar vortex, was less important than these other two mechanisms. For the ClO dimer mechanism to have been comparable to the cycle involving ClO and BrO, the ClO abundance must have been greater than 300 pptv, a number more than two times greater than that suggested by the OCIO column abundances observed by Solomon *et al.* (16). Of course, if ClO were highly localized in thin layers inside the vortex, then clearly the ClO dimer mechanism would have been more important there. Just outside the vortex, O<sub>3</sub> near 20 km was lost at a rate of 0.02% per day by catalysis involving ClO and BrO alone.

#### REFERENCES AND NOTES

1. J. C. Farman, B. G. Gardiner, J. D. Shanklin, *Nature* **315**, 207 (1985).
2. See, for example, the November 1986 supplementary issue of volume 13 of *Geophysical Research Letters*.
3. R. L. deZafra *et al.*, *Nature* **328**, 408 (1987); P. Solomon *et al.*, *ibid.*, p. 411; S. Solomon, G. H. Mount, R. W. Sanders, A. L. Schmeltekopf, *J. Geophys. Res.* **92**, 8329 (1987).
4. R. L. deZafra *et al.*, special issue of *J. Geophys. Res.* (1988); R. W. Sanders, S. Solomon, M. A. Carroll, A. L. Schmeltekopf, *ibid.*; S. Solomon, R. W. Sanders, M. A. Carroll, A. L. Schmeltekopf, *ibid.*

5. Results of Airborne Antarctic Ozone mission will appear shortly in a special issue of *The Journal of Geophysical Research*; J. G. Anderson, W. H. Brune, M. J. Proffitt, *ibid.*; W. H. Brune, J. G. Anderson, K. R. Chan, *ibid.*; J. G. Anderson *et al.*, *ibid.*, W. H. Brune, J. G. Anderson, K. R. Chan, *ibid.*
6. O. B. Toon, P. Hamill, R. P. Turco, J. Pinto, *Geophys. Res. Lett.* **13**, 1308 (1986); M. B. McElroy, R. J. Salawitch, S. C. Wofsy, *ibid.*, p. 1296; P. J. Crutzen and F. Arnold, *Nature* **324**, 651 (1986).
7. L. T. Molina and M. J. Molina, *J. Phys. Chem.* **91**, 433 (1986).
8. M. B. McElroy, R. J. Salawitch, S. C. Wofsy, J. A. Logan, *Nature* **321**, 759 (1986).
9. S. Solomon, R. R. Garcia, F. S. Rowland, D. J. Wuebbles, *ibid.*, p. 755.
10. Ozone Trends Panel Report, *NASA-WMO Spec. Publ.*, in press.
11. E. F. Danielsen and H. Houben, *J. Geophys. Res.*, in press.
12. M. P. McCormick, H. M. Steele, P. Hamill, W. P. Chu, T. J. Swessler, *J. Atmos. Sci.* **39**, 1387 (1982).
13. J. F. Noxon, *J. Geophys. Res.* **84**, 5067 (1979).
14. B. A. Ridley *et al.*, *ibid.* **89**, 4797 (1984).
15. G. H. Mount, S. Solomon, R. W. Sanders, R. O. Jakoubek, A. L. Schmeltekopf, *Science* **242**, 555 (1988).
16. S. Solomon, G. H. Mount, R. W. Sanders, R. O. Jakoubek, A. L. Schmeltekopf, *ibid.*, p. 550.
17. L. E. Heidt, private communication.
18. W. L. Starr and J. F. Vedder, in (5).
19. W. H. Brune, J. G. Anderson, K. R. Chan, in (5).
20. M. R. Schoeberl, private communication.
21. W. H. Brune, E. M. Weinstock, J. G. Anderson, *Geophys. Res. Lett.* **15**, 144 (1988).
22. U. Schmidt, R. Bauer, G. Kullessa, E. Klein, B. Schubert, presented at the Polar Ozone Workshop, Aspen, CO, 9 to 13 May 1988.
23. J. Rodriguez, private communication.
24. We thank N. L. Hazen, R. Kolyer, and R. Lueb for operating the instruments, and the management, staff, and pilots at Moffett Field who helped in every possible way, including flying on very short notice. The forecast weather maps provided by L. Bengtsson and the European Center for Medium Range Weather Forecasting and the NMC analyses provided by M. E. Gelman and the Climate Analysis Center made the directed flight possible. Conversations with J. M. Rodriguez, S. Lloyd, and M. R. Schoeberl are gratefully acknowledged. Supported by NASA contract NASW-3960 and NASA grant NAG2-526.

12 August 1988; accepted 19 September 1988

## Subattomole Amino Acid Analysis by Capillary Zone Electrophoresis and Laser-Induced Fluorescence

YUNG-FONG CHENG AND NORMAN J. DOVICH†\*

Subattomole analysis of fluorescein isothiocyanate (FITC) derivatives of amino acids is accomplished by combining capillary zone electrophoresis for high-efficiency separation with laser-induced fluorescence for high-sensitivity detection. Concentration detection limits range from  $5 \times 10^{-12}$  molar for alanine to  $9 \times 10^{-11}$  molar for lysine, injected in the column;  $9 \times 10^{-21}$  mole of alanine is contained within the  $\sim 1$ -nanoliter injection volume at the detection limit. The alanine detection limit corresponds to fewer than 6000 molecules injected onto the column and represents an improvement of four orders of magnitude in the state of the art for fluorescent detection of amino acids and an improvement of six orders of magnitude in the state of the art for the detection limit for isothiocyanate derivatives of amino acids.

ANALYSIS OF MINUTE QUANTITIES of amino acids is of broad interest. Because heroic efforts are often required to procure macroscopic quantities of biological samples, microanalysis schemes for amino acids are important. We report a relatively simple method for subattomole determination [1 attomole (amol) =  $10^{-18}$  mol] of the FITC derivative of amino acids. Although routinely used as a fluorescent label for proteins, FITC is less commonly used as a derivatizing reagent for amino acids; however, the derivatives are relatively easy to form, have good electrophoretic properties, and generate strong fluorescence signals (1–3). Our amino acid analysis is based on the combination of capillary zone

electrophoresis for the identification of amino acids with laser-induced fluorescence for detection of the amino acids. By this method, it is possible to determine subattomole quantities of 15 different FITC-amino acids in a 25-min separation period.

Capillary zone electrophoresis is an elegant technique for the separation of minute quantities of ionic species (4). In our instrument, a 99-cm length of fused silica capillary (inner diameter, 50  $\mu$ m) is used for the separation. Before the separation, the capillary is filled with 5 mM aqueous carbonate buffer, pH 10. Sample is introduced by dipping the positive end of the capillary tube into a small vial containing the sample; the power supply is connected to the vial with a platinum electrode, and a 2-kV potential is applied for 10 s. Under these conditions, an injection precision of a few percent is possible; the precision is limited primarily by the reproducibility in the length of time for

which the injection potential is applied. This injection technique introduces bias in the analysis; analytes with high electrophoretic mobility travel at a greater speed and thus are introduced to a greater extent than slower moving analytes. The results presented below have been corrected for this phenomenon (5). After injection, the sample vial is replaced by a vial containing the pH 10 buffer and high voltage is applied for separation of the amino acids. After each run, the high voltage is removed for a few minutes to allow the capillary to cool to ambient temperature. Although we have obtained separation efficiency of greater than 800,000 theoretical plates with a fresh capillary, the instrument more routinely produces 400,000 theoretical plates over a several month period.

Strong electroosmotic flow drives solvent from the positive to the negative end of the capillary; anions, cations, and neutral species may be detected in a single separation as they flow from the positive to the negative electrode. Detection occurs in a region after the capillary in a sheath flow cuvette (Fig. 1). This cuvette, commonly used in flow cytometry (6), provides good optical quality for high-sensitivity detection while virtually eliminating postcolumn band broadening that would degrade the separation performance; excellent laser-induced fluorescence detection limits have been achieved with this cuvette (7). In our system, the exit of the capillary tube is inserted into a quartz flow chamber 250  $\mu$ m by 250  $\mu$ m square. Sheath fluid, identical to the separation buffer, is introduced into the cuvette by a liquid chromatography pump at a flow rate of 9.3  $\mu$ L/min. To complete the electrical circuit for electrophoresis, the stainless steel plumbing associated with the sheath stream is held at ground potential. Under the very low flow rate produced by electroosmosis,  $\sim 40$  nL/min, the sample travels as a stream with a  $\sim 10$ - $\mu$ m diameter through the center of the cuvette. Fluorescence is excited by a light-regulated, 1-W argon ion laser beam focused to a 10- $\mu$ m spot about 0.2 mm downstream from the capillary exit. A laser wavelength of 488 nm both matches the absorbance spectrum of the FITC-amino acids (2) and provides a convenient spectral window wherein the fluorescence band falls between the excitation wavelength and the main water Raman band at 585 nm. Fluorescence is collected at right angles to both the sample stream and the laser beam with a 0.45 numerical aperture (NA), 18 $\times$  microscope objective. A 495-nm, long-wavelength pass colored glass filter is used to block scattered laser light, whereas a 560-nm, short-wavelength pass interference filter is used to block the Raman band of water. A

Department of Chemistry, University of Alberta, Edmonton, Alberta, Canada T6G 2G2.

\*To whom correspondence should be addressed.